

TECHNICAL PAPER

Local bond–slip model for plain surface reinforcement

John Cairns 

The School of Energy, Geoscience,
Infrastructure and Society, Heriot-Watt
University, Edinburgh, UK

Correspondence

John Cairns, The School of Energy,
Geoscience, Infrastructure and Society,
Heriot-Watt University, Edinburgh, UK.
Email: j.j.cairns@hw.ac.uk; civjic@hw.ac.uk

Abstract

Nowadays virtually all-concrete construction uses reinforcement with deformations rolled or indented on the bar surface to improve bond between bar and concrete, but many older structures built with plain surface bars remain in service. The increasing need for assessment of existing construction means there is a continuing need for information on their performance. Research into plain surface bars essentially ceased when ribbed bars became established, and plain bars have consequently been bypassed in developments in understanding and modeling of bond since 1960. The profession's ability to numerically model behavior of concrete structures has expanded dramatically since plain surface reinforcement was discontinued. The option of numerically modeling may be particularly important for assessment of existing structures with noncompliant details. Although the *fib* Model Code 2010 includes a local bond–slip model for plain surface bars, information on the derivation of the model and supporting evidence of its validation are not available. The current paper analyses data on bond–slip behavior of plain surface bars and demonstrates shortcomings in the *fib* model. An improved model is proposed and verified against test data from an independent source.

KEYWORDS

anchorage, assessment, bond slip, local bond, plain bars

1 | INTRODUCTION

Code committees have responded to the increasing requirement to verify capacity of existing structures by developing codes oriented toward assessment as well as new design. The American Concrete Institute (ACI) first published its Code Requirements for Evaluation, Repair, and Rehabilitation of Concrete Buildings in 2013.¹ The

version of EN1992 currently under development will include content on assessment, as will the *fib* Model Code 2020.²

Although reinforcement used today is invariably produced with ribs or indentations to improve bond between bar and concrete, many older structures reinforced with plain bars remain in service today. In the United Kingdom, for example, plain surface bars were the main type of reinforcement used prior to 1960 and in a significant number of structures constructed in the mid-70s when steel was in short supply due to industrial unrest. One estimate in 2002³ suggested that around 70% of existing construction in Italy was

Discussion on this paper must be submitted within two months of the print publication. The discussion will then be published in print, along with the authors' closure, if any, approximately nine months after the print publication.

This is an open access article under the terms of the Creative Commons Attribution License, which permits use, distribution and reproduction in any medium, provided the original work is properly cited.

© 2020 The Authors. Structural Concrete published by John Wiley & Sons Ltd on behalf of International Federation for Structural Concrete

reinforced with plain surface bars. A historical perspective on design provisions for plain surface bars in the United States shows variations in code requirements over time.⁴ It is sometimes advocated that assessment be based on code provisions at time of construction, but these variations could make conclusions of an assessment dependent on the assumed year of design, which might differ from that of construction. The new generation of assessment codes need to include information on properties and performance of obsolete materials such as plain surface bars.

A previous paper proposed expressions to estimate resistance of laps and anchorages of plain surface bars.⁵ The profession's ability to numerically model behavior of concrete structures has expanded markedly since plain surface reinforcement was discontinued. The option of numerically modeling may be particularly important for assessment of existing structures with noncompliant details.⁶ Although the *fib* Model Code (*fib* 2010) includes a local bond–slip model for plain surface bars, information on the derivation of the model and supporting evidence of its validation are not available. The current paper aims to develop a local bond–slip model to complement previous work on laps and anchorages to provide an improved representation of behavior. The scope of this paper is limited to plain bars in concrete of normal strength at time of construction stressed within the elastic range of the reinforcement and under monotonic loading.

2 | BOND MECHANISMS

The bond mechanism of plain surface bars differs from that of the ribbed bars in use today, which have been the subject of extensive research. Ribbed bars typically fail in bond through splitting of the concrete cover provided cover thickness does not exceed around 3–4 times bar diameter.⁷ Bearing of ribs on concrete is the major component of bond resistance of ribbed bars at the ultimate limit state, with capacity controlled by the resistance of the concrete cover to splitting, together with any additional restraint from transverse pressure and from confining reinforcement. Adhesion initially controls bond of plain bars but is broken at very low slips, and bar/concrete friction is generally considered the major component of bond resistance. Plain bars usually fail by pulling out of the concrete leaving cover uncracked. The mechanisms controlling bond behavior of plain surface bars therefore differ from those determining behavior of ribbed bars, and consequently a different bond–slip model is required to describe their behavior.

3 | LOCAL BOND–SLIP MODELS

Local bond–slip models are based on a “short” bond length, typically five times bar diameter and it is assumed that bond stress and slip may be considered uniform over that length. As such models are generally used to represent typical behavior rather than directly in design, they are derived for mean stresses and slip values. Models for ribbed bars have historically been derived first for “well confined” conditions in which concrete cover is of sufficient thickness to ensure a “pullout” failure mode in which the bar pulls out of the concrete leaving a smooth hole and without splitting the cover, although the *fib* Model Code 2010⁸ has extended its local bond–slip model to cover splitting failure modes.

The *fib* Model Code provides a model for both hot rolled and cold drawn plain surface bars composed of an initial nonlinear ascending portion and a horizontal plateau (Figure 1 and Table 1), but does not distinguish between “high” and “low” confinement, although it does distinguish between good and other bond conditions. A representative set of bond–slip plots for bars of various diameters from Abrams⁹ tests on bars concentrically embedded in cylindrical concrete prisms are shown in Figure 2. The cylinders were 8” (204 mm) in diameter in all cases. Bar diameter ranged from 6.3 to 32 mm and the embedment length varied between 12 and 12.8 times bar diameter. Average concrete cylinder compressive strength f_{cm} was 10.9 MPa. Bond–slip behavior is characterized by an initial stiff response until adhesion is broken, followed by a softening response until peak load is reached, and a subsequent gradual descent postpeak. The *fib* MC2010 representation, in comparison, shows a lower initial stiffness and slip at peak load. MC2010 shows no reduction in capacity once peak load is reached, whereas

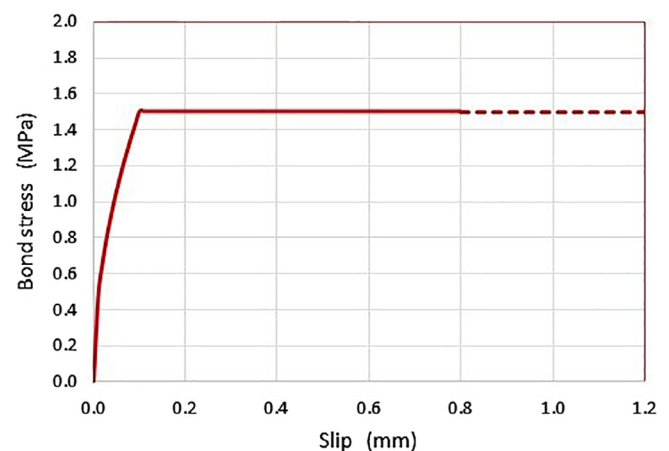
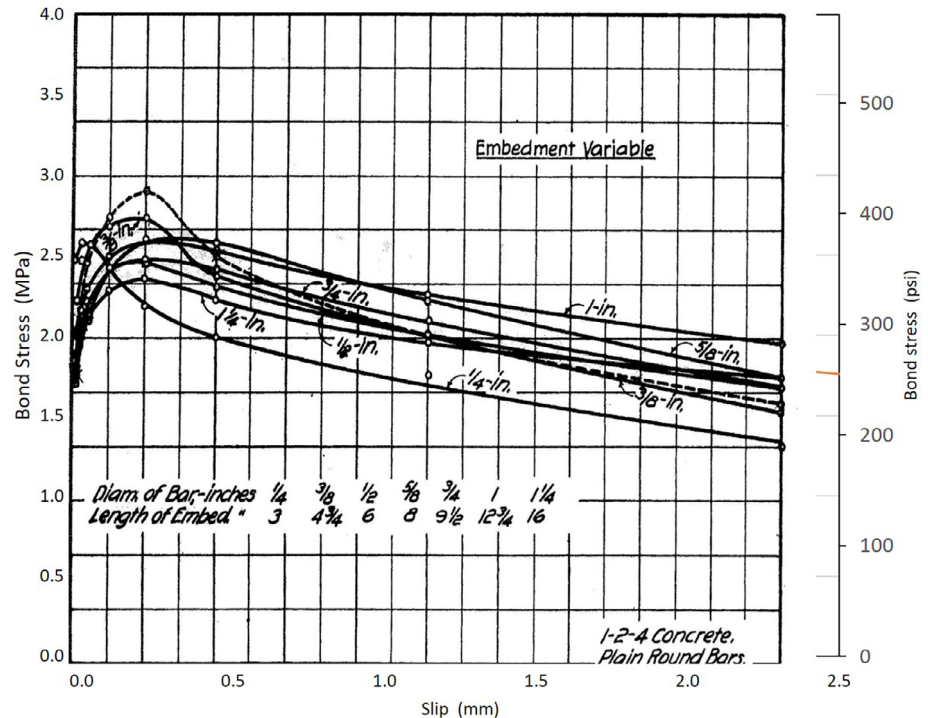


FIGURE 1 Local bond–slip model from *fib* Model Code 2010⁸

TABLE 1 Local bond–slip parameters from MC2010 Table 6.1-2

	Cold drawn wire		Hot rolled bars	
	Good bond conditions	All other bond cond.	Good bond conditions	All other bond cond.
$s_1 = s_2 = s_3$	0.01 mm	0.01 mm	0.1 mm	0.1 mm
α	0.5	0.5	0.5	0.5
$\tau_{bmax} = \tau_{bf}$	$0.1\sqrt{f_{cm}}$	$0.05\sqrt{f_{cm}}$	$0.3\sqrt{f_{cm}}$	$0.15\sqrt{f_{cm}}$

FIGURE 2 Local bond–slip plots from Abrams⁹

Abrams' tests show resistance at 2.5 mm slip is reduced by around one third below the peak value.

Verderame et al.⁶ have suggested a local bond–slip model for plain bars derived from their own test using a bond length of 10 times diameter, somewhat larger than desirable for local behavior. However, heat-laminated plain steel bars were used, which appear to have a brighter surface condition than that of hot-rolled bars, and which attained lower bond strengths than those measured by Abrams. Individual calibrations for each of the 10 tests conducted are reported. Feldman and Bartlet¹⁰ proposed a model based on their own tests using cold rolled and artificially roughened plain bars. A total of 252 tests were conducted with bond lengths from 12 to 48 diameters. Bond was very sensitive to surface roughness and peaked at a very low slip, typically of 0.01 mm or less, suggesting resistance was almost entirely attributable to adhesion and that the friction component active at higher slips was absent. Melo et al.¹¹ proposed a bond–slip relationship based on loaded end slips. Hot rolled bars were used “as

delivered” with mill scale largely intact. Three bar diameters were tested with bond lengths of 5, 30, and 45 times bar diameter. Two trends in their results are inconsistent with other studies. First, average bond strengths measured on 5ϕ bond lengths are lower than on those measured on 30 and 45 embedment lengths, the opposite trend to that reported by most investigations of bond and to well-established equivalent expressions for ribbed bars.⁷ Second, bond of 12 mm bars was weaker than that of the 10 mm and the 16 mm sizes, which also is at variance from the expected trend.

4 | DERIVATION OF MODEL FOR PLAIN ROUND BARS

4.1 | Selection of test data

A survey was conducted to identify existing studies on bond of plain surface bar¹², and to select from this body of work the test data on which a revised local bond–slip

model could be based. Several studies were rejected following an initial appraisal:

1. Tests on lapped joints in beams do not provide useful data as direct measurement of slip is not possible.
2. Tests on bars other than hot rolled, whether artificially roughened or not.
3. Studies which did not follow behavior after peak load.
4. Bond lengths of 15 diameters or more were considered too long to be helpful in calibration of a local model.
5. Investigations containing few results and covering a very limited range of parameters, which consequently were considered to carry little statistical weight.
6. Tests using specimens in which bars were anchored were preferred over transfer type tests in which bond stresses would be more strongly influenced by surrounding concrete.

As a result of the foregoing, it was decided to base analysis primarily on tests on round bars reported by Abrams⁹ in a very extensive investigation within which variable parameters included concrete strength, bond length, confinement from cover and transverse reinforcement and bar diameter, even though only a few tests were conducted on a 5-diameter bond length. These tests primarily used hot-rolled bars from normal production, although polished and rusted bars were included in a few minor subseries. In another very extensive investigation, Snowdon¹³ used 10 different specimen types, although fewer parameters were systematically varied. A bond length of 6 diameters was used in one specimen and this is considered particularly useful for validation as it is close to the 5-diameter bond length generally used for modeling of bond slip. Snowdon tested both plain round and square section plain bars as well as a variety of ribbed bars. A further benefit in using these two investigations is that Abrams conducted his study early in the history of reinforced concrete while Snowdon's work was carried out toward the end of the time when plain bars were extensively used.

4.2 | Evaluation of peak bond stress τ_{bmax}

As stated earlier, local bond-slip models have conventionally been based on a bond length of 5 diameters. Abrams tested a range of bond lengths from 3 to 20 times bar diameter, but 5-diameter bond lengths were used in only a small number of tests, which did not cover other major variables. Most tests used a bond length of around 12 diameters, that is, 2.4 times longer than the conventional 5 diameters. The evaluation proceeds by

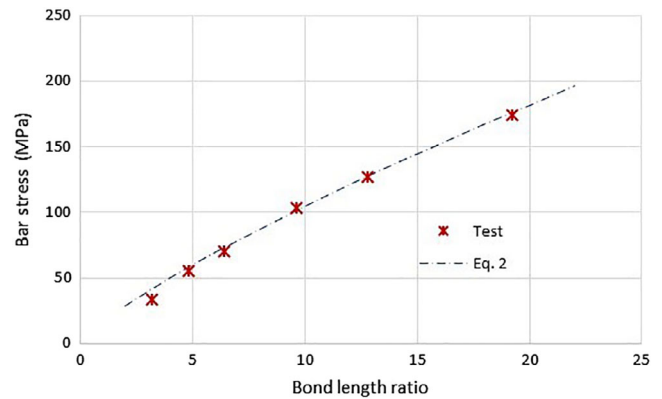


FIGURE 3 Variation in bar stress at peak load with bond length ratio, tests by Abrams⁹

considering the influence of bond length, cover ratio, and concrete strength successively to build an expression for τ_{bmax} . The sequence follows that selected by Palmisano et al.¹⁴ to obtain a fit to lap and anchorage data.

Figure 3 plots the variation in bar stress at peak load measured in tests by Abrams against bond length ratio l_b/ϕ . Bar stress is obtained from bond strength f_b reported by Abrams using Equation (1). Each point represents the mean of between 5 and 12 individual tests. These results were obtained from pullout type tests on 32 mm diameter bars axially embedded in 204 mm diameter concrete cylinders giving a minimum cover to diameter ratio of 2.7ϕ . Concrete strength averaged 9.7 MPa. The trend line giving a good fit to test data is shown dashed and is given by Equation (2). The ratio of the strength measured in tests to that estimated by Equation (2) averages 1.00 with a coefficient of variation of 0.09.

$$f_{stm} = 4f_b(l_b/\phi) \quad (1)$$

$$f_s = 16(l_b/\phi)^{0.8} \quad (2)$$

The index of 0.8 in Equation (2) shows the increase in stress anchored is less than proportional to the increase in bond length, and consequently that average peak bond-strength reduces with increasing bond length. The index of 0.8 on bond length ratio in Equation (2) equals that reported by Cairns and Feldman⁵ for laps. Note that the horizontal plateau in the MC2010 local bond-slip model for plain bars is inconsistent with the observed trend for reduced average bond strength with longer bond lengths.

An estimate for peak bond-stress τ_{b1} for a concrete strength of 9.7 MPa and 32 mm diameter bars as used in these tests is obtained by rearranging Equations (2) and (3).

$$\tau_{b1} = f_{s/4}(\nu_{\phi}) = 4(l_b/\phi)^{-0.2} \quad (3)$$

Abrams tested a range of bar diameters from 6.4 to 32 mm and observed a reduction in peak bond stress with increasing bar diameter (Figure 4). Tests were again conducted on bars axially embedded in 204 mm diameter concrete cylinders. There are only minor variations in bond length ratio within the range 12 and 12.8 times bar diameter for the series. The expression given in Equation (4) gives a reasonable fit to test data as shown by the dashed line in Figure 4. The ratio of the strength measured in tests to that estimated by Equation (4) averages 1.01 with a coefficient of variation of 0.04.

$$\tau_{b2} = 4.8 \phi^{-0.2} \quad (4)$$

Peak bond stress is influenced by concrete strength. MC2010 presents τ_{bmax} as proportional to the square root

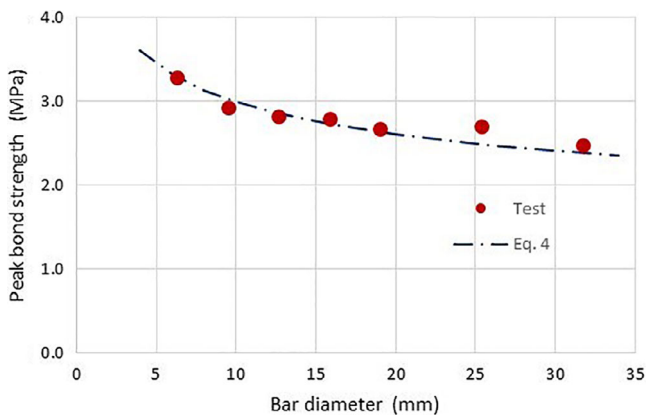


FIGURE 4 Variation in peak bond stress with bar diameter, tests by Abrams⁹

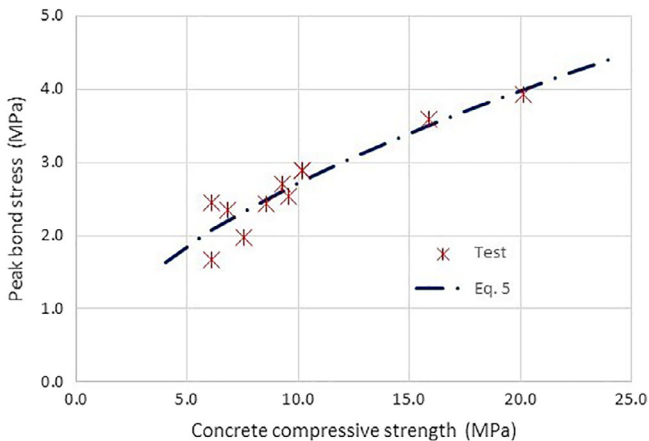


FIGURE 5 Variation in peak bond stress with concrete cylinder compressive strength, tests by Abrams⁹

of concrete strength. Cairns and Feldman confirmed this relationship from tests on laps and anchorages, while Palmisano et al.¹⁴ suggested bond is a function of $f_{cm}^{0.55}$. Abrams results for the variation in peak bond strength with concrete strength are plotted in Figure 5. Results are for 19.1 mm diameter bars axially embedded in 204 mm diameter cylinders with a bond length of 204 mm, equivalent to $l_b/\phi = 10.7$. Two of the results tabulated in the original report relate to mixes with little or no coarse aggregate and they have been disregarded. The trend line giving a reasonable fit to test data is shown dashed and is given by Equation (5). The ratio of the strength measured in tests to that estimated by Equation (5) averages 1.02 with a coefficient of variation of 0.10.

$$\tau_{b3} = 0.75 f_{cm}^{0.55} \quad (5)$$

Equation (3) was derived for 32 mm bars and a concrete compressive strength of 9.7 MPa and it must be modified to deal with a range of bar diameters and concrete strengths. Equation (6) proportions Equation (3) for other concrete strengths and diameters in accordance with the influence of these parameters as described by Equations (4) and (5).

$$\tau_{bmax} = 4(l_b/\phi)^{-0.2} (32/\phi)^{0.2} (f_{cm}/9.7)^{0.55} \quad (6)$$

For consistency with other parts of the *fib* Model Code, Equation (6) is recalibrated for a reference bar diameter of 25 mm and a concrete strength of 25 MPa, Equation (7).

$$\begin{aligned} \tau_{bmax} &= 4(l_b/\phi)^{-0.2} (25/\phi)^{0.2} (32/25)^{0.2} (f_{cm}/9.7)^{0.55} (25/9.7)^{0.55} \\ &= 6.9(l_b/\phi)^{-0.2} (25/\phi)^{0.2} (f_{cm}/25)^{0.55} \end{aligned} \quad (7)$$

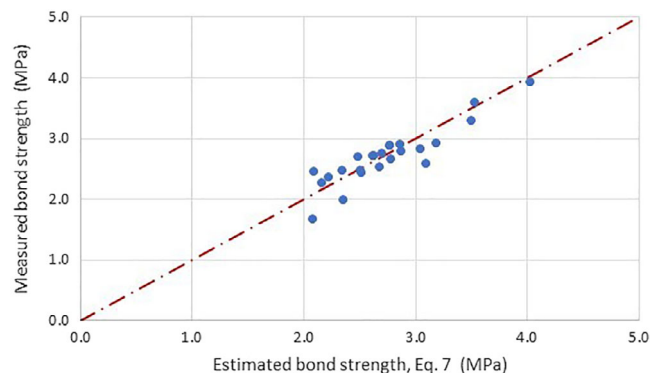


FIGURE 6 Comparison between measured bond strength and strength estimated by Equation (7)

Figure 6 compares measured bond strength with strength estimated by Equation (7). The measured/estimated ratio averages 0.99 with a coefficient of variation of 0.085 for all results used in calibration of Equations (2)–(7).

For the conventional local bond–slip bond length of 5ϕ , bond-length ratio l_b/ϕ in Equation (7) is set to five, giving Equation (8).

$$\tau_{bmax} = 5.0 \left(\frac{f_{cm}}{25} \right)^{0.55} \left(\frac{25}{\phi} \right)^{0.2} \quad (8)$$

For a 25 mm hot rolled bar in concrete with a mean compressive strength of 25 MPa in good bond conditions Equation (8) gives $\tau_{bmax} = 5.0$ MPa, compared with a value of 1.5 MPa in MC2010 (Table 1), and therefore shows the value for τ_{bmax} given in Table 6.12 of MC2010 is very conservative.

4.3 | Other model parameters

Bond–slip relationships for various bar diameters (Figure 2) show free end slip s_1 at peak load to generally lie between 0.2 and 0.3 mm with an average of around 0.25 mm for most diameters. Only the smallest 1/4" (6 mm) diameter bar shows a marked difference with a slip at peak load of below 0.05 mm. The anomalous result for 6 mm bars is ignored, as such a small diameter is unlikely to figure in the major assessment in which numerical modeling would be employed. Abrams' own analysis of bond–slip plots for 32 mm bars over a range of bond lengths from 3.2 to 19.2 diameters shows peak bond for a "very short" bond length is reached at a slip of 0.25 mm. Other results in Abrams report do not show any significant variation with either concrete mix or storage conditions. Slips s_1 as low as 0.012 mm and up to 0.5 mm were observed in some test series, but mainly for the highest or lowest value of the parameter under investigation in the series, and there appears to be no systematic variation across the whole range of values. Snowdon's results similarly show slip s_1 to lie between 0.25 and 0.40 mm. Residual strength at 2.5 mm slip, the maximum shown in Abrams' results, is around 60% of peak value. Snowdon shows no results for slips greater than 1.0 mm, at which stage bond stress had dropped back by 11% on average. Abrams detected first slip at 0.025 mm, which he considered to represent the limit of adhesion bond. This was reached when the applied bond stress was around 60% of the peak value reached in the test. Snowdon reports bond stress at a slip of 0.025 mm to be 66% of τ_{bmax} .

4.4 | Proposed model for good bond conditions

The local bond–slip relationship proposed here comprises two segments, a rising segment and a descending segment. The same form of expression is used for both segments, and the lesser of the two values is selected. The form of expression is identical to that of the initial segment for ribbed bars given in MC2010.⁸

$$\tau_b = \tau_{bmax} \left(\frac{s}{s_1} \right)^\alpha \quad (9)$$

For $0 \leq s \leq s_1$, based on the relationship that $\tau_b \approx 0.6 \tau_{bmax}$ when $s = s_1/10$, $\alpha_r = 0.2$ provides a reasonable representation of the ascending branch.

For slip $s > s_1$, a value $\alpha_f = -0.2$ is adopted giving a residual bond stress equal to 63% of the peak value when $s = 10s_1$.

Figure 7 compares the proposed local bond–slip model (plotted by a red chain-dashed line) with measured bond slips from Abrams. Peak bond strength τ_{bmax} is obtained from Equation (7) with $\phi = 19$ mm, the arithmetic mean of the maximum and minimum diameters on the plot, a bond length ratio of 12.4 times bar diameter and a concrete compressive strength of 10.9 MPa as in the original tests. The model lies within the range of test observations for diameters between 6.35 and 32 mm, although the transition between ascending and descending branches is somewhat peakier than observed experimentally.

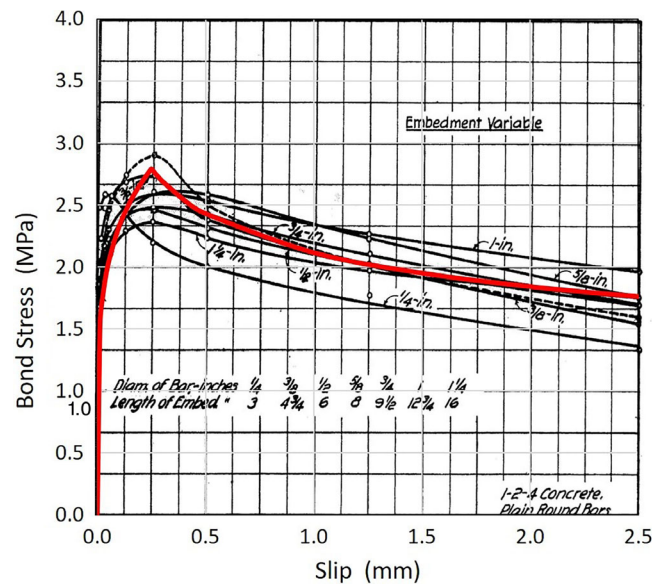


FIGURE 7 Comparison between proposed local bond–slip model and measurements by Abrams⁹

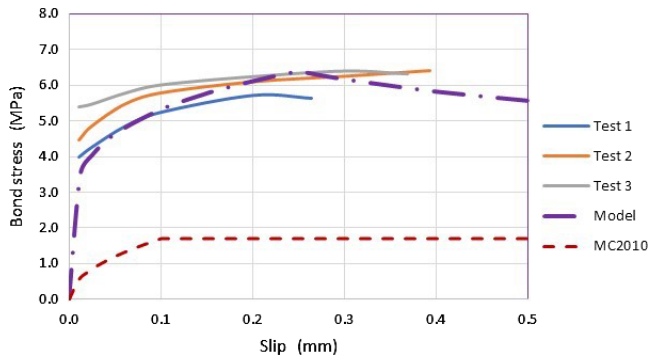


FIGURE 8 Comparison between proposed local bond-slip model and measurements by Snowdon¹³

A further independent verification is provided in Figure 8 where the predictions of Equation (7) are compared with results from three sample tests from 12 summarized by Snowdon¹³ for pullout type specimens with a bond length of 6 diameters. Although he conducted a large number of tests with a variety of specimens and bars and reports broadly consistent behavior throughout his investigation, detailed bond-slip plots are presented for few tests with a “short” bond length. Bar diameter was ½” (12.7 mm) and concrete cube strength was 40.4 MPa, taken as equivalent to a mean cylinder strength of 32.3 MPa. The proposed relationship lies within the range of experimental variations. Figure 8 also shows the corresponding bond stress-slip relationship given by MC2010 for the same concrete strength. It is evident that the MC2010 model greatly underestimates the bond stress and stiffness, which plain round bars can develop.

4.5 | Comparison with semi-empirical analysis of lap and anchorage strength

Cairns and Feldman⁵ analyzed results from several investigations to derive an expression for strength of laps and anchorages of plain bars, Equation (10). The indices on concrete strength and bond length ratio in Equation (10) are almost identical to those for the corresponding parameter in Equations (2) and (5) herein. Bar size appears as a parameter in Equation (7) but not in Equation (10). Conversely, Equation (10) includes minimum cover ratio whereas Equation (7) does not. Cairns and Feldman⁵ noted a strong inverse cross correlation between bar size and minimum cover ratio c_{min}/ϕ in their analysis, which precluded evaluation of its influence. The range of bar sizes in their study was also lower than in Abrams’ investigation.

$$f_s = 11.2\eta_2(f_{cm}/25)^{0.5}\left(c_{min}/\phi_{eq}\right)^{0.65}\left(l_b/\phi_{eq}\right)^{0.8} \quad (10)$$

The maximum value of c_{min}/ϕ in Cairns & Feldman’s database was 3.0 and this was proposed as a limit to the permissible value to be used in Equation (10). Substituting $c_{min}/\phi = 3.0$ in Equation (10) and setting $\eta_2 = 1.0$ for a “good” casting position leads to Equation (11a). Bar diameter in their database had a median value of 25 mm. Substituting this value into Equation (7) and substituting Equation (7) into Equation (1) leads to Equation (11b). The form of Equations (11a) and (11b) is identical and values of indices on concrete strength and bond length ratio are similar, although Equation (11b) derived for peak bond strength in pullout specimens gives values 20% higher than Equation (11a) derived for laps and anchorages. Cover was higher in the pullout specimens than in lap and anchorage tests and compression stress “cones” from the bearing face of pullout specimens would also have generated radial stresses on the bar concrete interface. Both would tend to enhance bond capacity of bars in pullout specimens compared to lap/anchorage specimens of otherwise similar parameters. It is concluded that, as far as can be ascertained from available test data, Equations (7) and (10) are consistent for “confined” conditions.

$$f_s = 22.9(f_{cm}/25)^{0.5}\left(l_b/\phi_{eq}\right)^{0.8} \quad (11a)$$

$$f_s = 27.6(f_{cm}/25)^{0.55}\left(l_b/\phi\right)^{0.8} \quad (11b)$$

4.6 | Comparison with other bond-slip models

Table 2 provides a snapshot comparison of values for key parameters in individual models for bond slip proposed by others including Verderame et al.,⁶ Feldman and Bartlett,¹⁰ Melo et al.,¹¹ MC2010 as well as the current proposal. As the various proposals use different expressions to evaluate these parameters, values given in Table 2 are calculated for a specific set of parameters, namely a bond length of 5 diameters, a bar diameter of 16 mm, concrete compressive strength of 20 MPa, and a reinforcement yield strength of 400 MPa. The descending part of the relationship is quantified here by $\tau_{b2.5}$, bond stress at a free end slip of 2.5 mm calculated according to each model.

Melo et al., the only other study in Table 2 to have used hot-rolled bars, and the current proposal both indicate a value for slip s_1 at peak load around 0.25 mm, which can be considered consistent given the difficulty of accurately determining peak value at the top of a curve.

TABLE 2 Comparison of key parameters from local bond–slip models for 5ϕ bond length, $f_c = 20$ MPa, $\phi = 16$ mm, $f_y = 400$ MPa

	Bar type/finish	α	τ_{bmax} (MPa)	$\tau_{bmax}/\sqrt{f_c}$	s_1 (mm)	τ_f (MPa)	$\tau_{b2.5}$ (MPa)	$\tau_{b2.5}/\tau_{bmax}$
MC2010	Hot rolled	0.50	1.34	0.30	0.10	1.34	1.34	1.00
	Cold rolled	0.50	0.45	0.10	0.01	0.45	0.45	1.00
Verderame et al.	Heat laminated	0.26	1.39	0.31	0.23	0.60	0.60	0.43
Melo et al.	Hot rolled	0.09	2.29	0.51	0.23	0.94	1.67	0.73
Feldman and Bartlett	Cold rolled	–	1.47	0.33	0.01	0.31	0.54	0.37
	Std. sandblast	–	2.75	0.61	0.01	0.56	1.00	0.36
	High sandblast	–	3.98	0.89	0.01	0.79	1.43	0.36
Proposal Equation (8)	Hot rolled	0.20	4.84	1.08	0.25	–	3.05	0.63

The difference in the ratio $\tau_{b2.5}/\tau_{bmax}$ between the current proposal and that of Melo et al lies within the scatter in test data. There is, however, a large difference in the value of τ_{bmax} between the two studies based on hot-rolled bars, with Equation (8) estimating peak bond strength more than double that of Melo et al. While the reason for this difference cannot be identified, two points should be made: first, the proposal presented here derives from tests conducted using the materials current when plain bars were in common use. Secondly, there are inconsistencies between trends in the model of Melo et al and other evidence, particularly the low bond strength for 5ϕ bond lengths compared to those for 30ϕ and 45ϕ .

Table 2 shows lower but similar values of τ_{bmax} and $\tau_{b2.5}$ for the cold rolled bars tested by Feldman and Bartlett and the heat-laminated bars tested by Verderame et al. but slip at peak load shows a significant difference. Feldman and Bartlett’s model is consistent with results from Abrams, who noted that polished bars had a lower peak bond capacity than normal hot rolled bars. Sandblasted bars tested by Feldman and Bartlett show values of τ_{bmax} between those for hot-rolled and cold rolled bars, a postpeak residual capacity half that for rolled bars, and a very much lower slip at peak load, generally consistent with stronger adhesion and lower friction components.

Three investigations all report a value for exponent α , well below the 0.5 in MC2010 and markedly greater peak bond strength. All show a descending branch rather than a level plateau.

5 | OTHER CONDITIONS AND BAR TYPES

5.1 | Minimum cover

Neither the work of Abrams⁹ nor pullout tests by Feldman and Bartlett¹⁰ show a systematic variation in

peak bond resistance with minimum cover. As stated above, however, Cairns and Feldman⁵ analyzed results from several investigations and noted that minimum cover appears to exert a marked influence on strength of laps and anchorages. Results examined in this study are taken from pullout specimens, which subject bars to a very different stress environment from laps and anchorages in normal construction.¹⁵ It seems likely that minimum cover would influence the value of τ_{bmax} , but available results do not allow this to be evaluated.

5.2 | Casting position

The parameters used to define “good” and “poor” casting positions in MC2010 have been derived from investigations on ribbed bars but should also be broadly appropriate for plain bars. Conventional pullout tests in which a vertical bar is concentrically cast in concrete provide no information on the influence of casting position. Cairns and Feldman⁵ report an analysis of tests on lapped joints in beams and beam end type specimen in which hot rolled plain round bars were cast in either top or bottom of the specimen and concluded that bond strength of top cast bars averaged around 50% of the corresponding bottom cast bars. It therefore seems reasonable to reduce the lead coefficient in Equation (8) by the same proportion for “poor” casting positions.

5.3 | Plain square bars

Equation (7) has been derived for plain surface bars of circular cross section. Plain bars of square section or square with chamfered corners have also been used as reinforcement in the past. From an analysis of tests on laps and anchorages Cairns and Feldman⁵ suggested it

would be reasonable to use the same strength expression for both section shapes but using the equivalent diameter of a square section bar. Feldman and Bartlett¹⁰ conducted pullout tests, which provide a direct comparison between the two section shapes. No systematic difference in peak bond resistance is apparent from the results reported. The equivalent diameter of a square section bar is less than 13% greater than that of its size, and it is unsurprising that the scatter in the ratio of peak bond resistance of round to square does not allow any firm conclusion to be drawn.

5.4 | Cold drawn bars and wires

Cold drawn bars and wires have a smoother surface than hot rolled bars. Slip at peak load is less than for hot rolled bars and peak resistance is also lower (Table 2). Abrams reports that cold rolled “tool steel” had around 65% of the bond strength of hot rolled bars tested under similar conditions. Were such bars polished before casting, bond resistance further reduced to 55%. Slip at peak load reduced to around 0.01 mm. Feldman and Bartlett report a similar slip at peak load for their tests on cold drawn bars (Table 2). It appears that the smoother cold drawn bars are largely dependent on adhesion, which is broken at a very low slip and that little additional frictional resistance capacity is available once slip starts.

Cold drawn reinforcement was limited to smaller bar sizes (typically 12 mm diameter or less) when plain surface bars were in common use, and consequently are unlikely to be critical elements in structural elements large enough to merit detailed numerical modeling in assessment.

5.5 | Initially corroded bars

Corrosion prior to concreting increase surface roughness and hence increases the frictional component of bond resistance. Abrams found a “heavy coat of firm rust” increased peak bond strength by around 15%, with

maximum bond resistance at around 0.35 mm, 40% higher than for mill surface bars. Murphy¹⁶ also reports that moderate surface corrosion results in an increase in bond resistance. Normal levels of compaction, perhaps combined with the high alkalinity of fresh cement paste, appear sufficient to clean light rust from a bar. Only flaking rust was found to cause a significant reduction in bond.

6 | CONCLUSIONS AND RECOMMENDATIONS

Increasing demand for assessment of existing construction has generated a need for data on performance of obsolete materials. This study proposes a new local bond–slip relationship for plain surface bars representative of production in the early part of the 20th century. The relationship has additionally been validated against tests on bars from the mid-20th century, around the time when plain bars were being phased out of typical construction and ribbed deformed bars became the norm.

Concrete strength, bar size, and bond length have been found to influence peak bond strength and hence also the local bond–slip relationship. Minimum cover ratio may also be a parameter but available test data do not allow its influence to be separated from that of bar size. Further tests are required to quantify and understand the influence of minimum cover on the local bond–slip relationship.

For monotonic loading the value τ_b of the bond stress between concrete and reinforcing bar can be calculated as a function of the displacement s of the bar parallel to the bar axis relative to the adjacent concrete. Values for parameters s_1 , α_r , and α_f are given in Table 3.

$$\tau_b = \tau_{bmax} \min \left[(s/s_1)^{\alpha_r}, (s/s_1)^{\alpha_f} \right] \quad (12)$$

The peak bond strength in the proposed local bond–slip model is shown to be broadly consistent with expressions

TABLE 3 Parameters defining the bond stress–slip relationship of hot-rolled plain surface bars in well-confined conditions

	Hot rolled bars		Cold drawn bars and wires	
	Good bond conditions	All other bond conditions	Good bond conditions	All other bond conditions
s_1	0.25 mm	0.25 mm	0.02 mm	0.02 mm
α_r	0.2	0.2	0.2	0.2
α_f	−0.2	−0.2	−0.2	−0.2
η_4	$5.0 (25/\emptyset)^{0.2}$	$2.5 (25/\emptyset)^{0.2}$	$2.5 (25/\emptyset)^{0.2}$	$1.25 (25/\emptyset)^{0.2}$
τ_{bmax}	$\eta_4 \sqrt{f_{cm}/25}$			

for mean strength of laps and anchorages in “good” casting position proposed in other studies, although it is higher than in one other proposal.¹¹ Some trends observed in the data on which that model was derived appear questionable, however. Nonetheless, in any practical application it would be prudent to assess sensitivity of the outcome to a reduction in the value of τ_{bmax} given in Table 3 pending additional test data.

The proposed local bond–slip model has been derived for bars with a hot-rolled mill scale surface in a “good” casting position and “confined” conditions. Cold drawn bar and wire has a smoother surface and shows a lower value for τ_{bmax} , which is reached at a lower slip. Conversely bars which have become lightly rusted exhibit a higher value for τ_{bmax} , which is reached at a greater slip. The proposed model will therefore be conservative for bars with light to moderate corrosion.

The influence of bar section shape is unclear, but given the sensitivity of bond–slip behavior of plain bars to surface condition, is probably not significant for practical purposes.

The peak bond strength given in the local bond slip model in the *fib* Model Code 2010 appears to be conservative, but the descending branch is not represented.

ORCID

John Cairns  <https://orcid.org/0000-0001-9886-3661>

NOTATION

c_{min}	minimum concrete cover to reinforcing bar
f_{cm}	compressive strength of concrete (mean value)
f_b	bond strength measured in test
f_s	estimated stress in reinforcing bar
f_{stm}	measured stress in reinforcing bar (mean value)
l_b	bond length between bar and concrete
s	relative slip between bar and concrete
s_1, s_3	slip at peak load and slip at end of descending branch respectively
α_r, α_f	parameters in the local bond–slip model
ϕ, ϕ_{eq}	diameter of round bar, equivalent diameter of square section bar
η_2	coefficient for casting position
τ_b	bond stress
τ_{b1}	estimates of peak value of bond stress for specific sets of parameters
τ_{b2}, τ_{b3}	specific sets of parameters
τ_{bmax}	peak value of bond stress
$\tau_{b2.5}$	bond stress at free end slip of 2.5 mm

ORCID

John Cairns  <https://orcid.org/0000-0001-9886-3661>

REFERENCES

1. ACI Committee 562. Code requirements for evaluation, repair, and rehabilitation of concrete buildings. Farmington Hills, MI: American Concrete Institute, 2013;p. 59.
2. *fib* Model Code 2020. [in preparation].
3. Fabbrocino G, Verderame GM, Manfredi G, Cosenza E. Experimental behaviour of anchored smooth rebars in old type reinforced concrete buildings. *Eng Struct.* 2002;27:1575–1585.
4. Feldman LR, Cairns J. Assessing historical provisions for the bond of plain bars. *ACI Struct J.* 2017;114(2):463–472.
5. Cairns J, Feldman LR. Strength of laps and anchorages of plain surface bars. *Struct Concr.* 2018;19:1782–1791.
6. Verderame GM, De Carlo G, Ricci P, Fabbrocino G. Cyclic bond behaviour of plain bars. Part II: Analytical investigation. *Constr Build Mater.* 2009;23:3499–3522.
7. *fib*. Bond and anchorage of embedded reinforcement: Background to the *fib* Model Code 2010. Technical Report 161; 2014.
8. *fib*. *fib* Model Code 2010. Berlin: Ernst & Sohn, 2013.
9. Abrams DA. Tests of bond between concrete and steel. Urbana, IL: University of Illinois at Urbana-Champaign, 1913.
10. Feldman LR, Bartlett M. Bond strength variability in pullout specimens with plain reinforcement. *ACI Struct J.* 2005;102(6):860–867.
11. Melo J, Rossetto T, Varum H. Experimental study of bond-slip in RC structural elements with plain bars. *Mater Struct.* 2015;48:2367–2381.
12. Feldman L, Cairns J. Plain Bar Literature Summary for *fib* TG4.5. Private communication; 2012.
13. Snowdon LG. Classifying reinforcing bars for bond strength. Watford, UK: Building Research Establishment, 1970.
14. Palmisano F, Greco R, Biasi M, Tondolo F, Cairns J. Anchorage and laps of plain surface bars in R.C. structures. *Eng Struct.* 2020;213. <https://doi.org/10.1016/j.engstruct.2020.110603>.
15. Cairns J, Plizzari G. Towards a harmonised European bond test. *Mater Struct.* 2003;36(262):498–506.
16. Murphy FG. The effect of initial rusting on the bond performance of reinforcement, CIRIA Report 71. London: CIRIA, 1977.

AUTHOR BIOGRAPHY



John Cairns, The School of Energy, Geoscience, Infrastructure and Society, Heriot-Watt University, Edinburgh, UK.

How to cite this article: Cairns J. Local bond–slip model for plain surface reinforcement. *Structural Concrete.* 2020;1–10. <https://doi.org/10.1002/suco.202000114>